Title

The Improvement of Cryogenic Mechanical Properties of Fe-12Mn and Fe-8Mn Alloy Steels Through Thermal/Mechanical Treatments

Authors

Hwang, S K
Morris, J W

Publication Date

1978-03-01

Submitted to Metallurgical Transactions

LBL-6618 Rev.
Preprint

THE IMPROVEMENT OF CRYOGENIC MECHANICAL PROPERTIES OF Fe-12Mn AND Fe-8Mn ALLOY STEELS THROUGH THERMAL/MECHANICAL TREATMENTS

S. K. Hwang and J. W. Morris, Jr.

March 1978

Prepared for the U. S. Department of Energy
under contract No. W-7405-ENG-48 and for the
National Aeronautics and Space Administration
under contract No. NASA-NGR-05-003-562

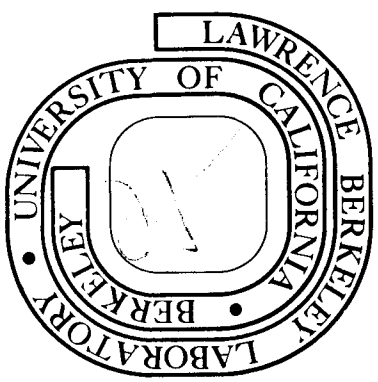

DISCLAIMER

LBL 6618 Revised

THE IMPROVEMENT OF CRYOGENIC MECHANICAL PROPERTIES OF Fe-12Mn AND Fe-8Mn ALLOY STEELS THROUGH THERMAL/MECHANICAL TREATMENTS

S.K. Hwang and J.W. Morris, Jr.

Department of Materials Science and Mineral Engineering and Materials and Molecular Research Division, Lawrence Berkeley Laboratory, University of California, Berkeley, CA 94720.

ABSTRACT

An investigation has been made to improve the low temperature mechanical properties of Fe-8Mn and Fe-12Mn - 0.2 Ti alloy steels. A reversion annealing heat treatment in two phase ($\alpha + \gamma$) region along with cold working has been identified as an effective treatment. In an Fe-12Mn-0.2Ti alloy a promising combination of low temperature ($-196^{\circ}C$) fracture toughness and yield strength was obtained by this method. These improvements of properties were mainly attributed to the ultra-fine grain size and to a uniform distribution of retained austenite (γ). It was also shown that an Fe-8Mn steel could be grain-refined by a purely thermal treatment because of its dislocated α' martensitic structure and absence of ϵ martensite. As a result, a significant reduction of ductile to brittle transition temperature was obtained in this alloy.

I. INTRODUCTION

Recent advances in cryogenic technologies have stimulated the production of specialty steels in large quantities. This creates a problem of consuming costly nickel, one of the major additions to the cryogenic iron alloys. The problem may be solved either by minimizing the nickel content in the commercial Fe-Ni steels or by developing a Ni-free cryogenic steel. In both approaches a common obstacle to overcome is to prevent the brittleness arising from the reduction of Ni which is believed to impart inherent toughness to Fe.[1-2]

A promising system for the development of a Ni-free cryogenic steel is Fe-Mn. Except for the formation of hcp ε martensite Mn affects the transformation behavior of the Fe lattice in much the same way that Ni does. Therefore, theoretically, the processing techniques utilizing the phase transformation of e.g., an α' martensitic Fe-Ni steel, should also be applicable to an Fe-Mn alloy of essentially the same structure.

Two metallurgical processing techniques have been identified so far to enhance the cryogenic toughness of ferritic Fe-Ni steels; grain size reduction and introduction of retained γ. It was found by Marschall et al.[3] that a heat treatment within two phase (α + γ) region was effective in achieving fine grain size and retained γ in a bcc 9Ni steel. The development of 6Ni steel by Nagashima and co-workers[4-5] was possible through modifying the alloy chemistry and heat treatment to give uniform and stable distribution of retained γ phase. Apart from the commercial alloys, it was shown by Jin et al.[6] that an alternate heat treatment in γ region and α +γ region yielded an extremely fine grain size in Fe-12Ni-0.25 Ti alloy. Later, Hwang[7] confirmed the beneficial effect of retained γ on the cryogenic impact toughness in this grain-refined alloy. However, the corresponding K_{IC} values did not show much

improvement over 100% bcc matrix, which was attributed to the low stability of the retained γ in this case.

The information on processing techniques to improve the quality of Fe-Mn alloys is scanty. Bolton et al.[8] studied the tempering effect on binary Fe-Mn alloys with varying Mn content from 4% to 10%*. While the tempering treatment was shown to be beneficial for low temperature toughness no retained phase (γ or ε) was observed in their work. Roberts[9] showed that the mechanical properties of Fe-Mn alloys containing up to 9% Mn were strongly influenced by the grain size and the substructure of transformation product. Schanfein[10] attempted to reduce the grain size of an Fe-8Mn alloy but was able to obtain only a minor suppression of ductile to brittle transition temperature.

The present investigation was aimed at obtaining better cryogenic mechanical properties in Fe-Mn alloys by applying the techniques successfully developed in Fe-Ni alloys. Fe-12Mn and Fe-8Mn were chosen for the base compositions since the former showed the lowest ductile-brittle transition temperature at a high martensitic strength[10] while the latter was most similar in microstructural features to those of α' martensitic Fe-Ni alloys.

In an Fe-12Mn-1.2 Ti alloy the improved cryogenic mechanical properties were obtained chiefly through grain size reduction and introduction of retained γ by heat treating the alloy within two phase (α + γ) region. The amount and the morphology of the retained γ were controlled by adding a cold working process prior to the two phase heat treatment. As a result an excellent combination of strength and toughness was obtained in this alloy. In an Fe-8Mn alloy the thermal cycling technique was found to be very effective in reducing grain size. Consequently the initial brittleness of this alloy was significantly suppressed.

---

* All in weight percent unless specified otherwise.

II. EXPERIMENTAL PROCEDURE

Ingots of Fe-8Mn and Fe-12Mn alloys with minor additions of Ti were induction melted in an argon gas atmosphere and cast into copper chill mold. The chemical compositions of the alloys are shown in Table I. Ti content in the 8Mn alloy turned out to be considerably less than that of 12Mn alloy presumably due to loss during melting process.

The cast ingots (approximately 9 kg each) were vacuum homogenized at 1200°C for 24 hours. These were then upset cross-forged at 1100°C and finish rolled into plastes of 2.5 cm thickness. A plate of 5 cm thickness was also made to obtain K_{IC} specimens after cold working. The plates were cut into blanks and subject to austenitizing treatment which consisted of 2 hours soaking at 900°C followed by ice brine quenching. The austenitized blanks underwent either heat treatment alone or cold working and heat treatment. The cold working was carried out at room temperature by rolling the blanks along the original rolling direction of plate. The thickness reduction in this process was 50%.

Specimens for mechanical testing were cut and machined from the heat treated blanks. For tensile testing sub-sized cylindrical specimens of 12.7 mm gage length and 3 mm gage diameter were used. The loading direction in the tensile test was parallel to the rolling direction of plate. A strain rate of 0.04/min. was employed. The uniform elongation was determined from the engineering stress-strain curves by measuring the strain following yielding until the stress reached the ultimate tensile strength. ASTM standard specimens were used for Charpy (V-notched) and K_{IC} (compact tension) tests. Charpy specimens were cut lengthwise along the rolling direction and the notches were machined on rolled-surface of plate. The loading direction in K_{IC} test was parallel to the rolling direction. The ductile to brittle transition

temperature in Charpy tests was determined as the temperature at which the impact energy value becomes equivalent to a half of the difference between upper and lower shelf energy. When specimens showed no sharp transition only their fracture modes at -196°C were examined under scanning electron microscope.

The phase transformation temperatures on continuous heating and cooling were measured by dilatometry using a heating rate of 440°C/min. and a cooling rate of approximately 70°C/sec. The results are shown in Table II. A typical dilation curve for an Fe-12Mn specimen is shown in Fig. 1.

The phase analysis was carried out using X-ray diffraction technique with Cu-K_α radiation. The volume percent of each phase present was calculated by comparing integrated intensities of $(200)_\alpha$, $(200)_\gamma$ and $(10\bar{1}1)_\epsilon$ peaks. However the results obtained by this method may be semiquantitative particularly in the presence of texture. In present work all the analyses were done on the transverse sections perpendicular to rolling direction. When compared to a magnetic saturation measurement[11] this method overestimated the amount of retained γ by approximately 8 vol. % in one sample (cold worked +600°c/4 hrs).

Microscopies (optical, SEM and TEM) were conducted by conventional laboratory techniques. The etchant used for the optical microscopy was picral and the jet-polishing solution for the TEM was chromic-acetic solution (75 g CrO_3 + 400 ml CH_3COOH + 21 ml H_2O).

III. EXPERIMENTAL RESULTS

Various heat treatments used in this work are summarized as follows.

Austenitizing; 900°C/2 hrs, standard treatment for all specimens.

Reversion annealing; for 12Mn alloy, heat treatment below $A_{f\alpha}$, ($\alpha' \rightarrow \gamma$ transformation finish temperature on heating).

Cold work and reversion annealing; for 12Mn alloy, 50% thickness reduction by cold rolling followed by the reversion annealing.

γ-cycling; for 12Mn alloy, heat cycling between γ region (680°C/5 min.) and ambient temperature.

γ, $\alpha + \gamma$ cycling; for 8Mn alloy, alternate heat treatment between γ region (750°C/2hrs) and $\alpha + \gamma$ region (650°C/2 hrs) with intermittent quencing to ambient temperature.

A. As-Quenched Structure.

A prior austentite grain size of approximately 70 μm was obtained in both Fe-12Mn-0.2Ti and Fe-8Mn alloys by austenitizing treatment followed by quenching. While no other than bcc phase was detected in the 8Mn alloy by X-ray diffraction measurement approximately 15 vol. % of hcp ϵ martensite was identified in the 12Mn alloy. The substructures of the two alloys are shown in Fig. 2. The martensite morphology of the 8Mn alloy was typical lath structure with high dislocation density. On the other hand the 12Mn alloy showed two different morphologies of martensite as denoted "A" and "B" in Fig. 2(b). The ϵ martensite was often observed along the boundaries of the block-like region "A". An example of a TEM dark-field contract of ϵ martensite is shown in Fig. 3 with diffraction pattern analysis.

The mechanical properties of the as-quenched alloys are shown in Table III. While the yield strength of the 8Mn alloy at -196°C was slightly higher than that of 12Mn alloy the latter showed significantly larger work hardening than the former. The Fe-12Mn alloy also showed better tensile ductility. The ductile to brittle transition in Charpy tests occurred sharply at 30°C and

$-50^{\circ}C$ in the 8Mn and the 12Mn alloy respectively. There was a clear difference in the low-energy fracture modes of the two alloys. As shown in Fig. 4 the brittle fracture occurred intergranularly along prior γ grain boundaries in the 12Mn alloy whereas a transgranular quasi cleavage mode was predominant in the 8Mn alloy. Above the transition temperature both alloys showed a ductile void growth and coalescence type fracture mode.

B. Fe-12Mn-0.2Ti. Effect of Reversion Annealing Treatment.

When a quenched martensitic Fe-Ni alloy is reheated and held at a temperature below As_{α} ($\alpha' \rightarrow \gamma$ transformation start temperature) $\alpha' \rightarrow \alpha + \gamma$ transformation occurs by equilibrium decomposition. The reverted γ may become stabilized by solute enrichment and grain size effect. The untransformed γ during subsequent cooling is referred to "retained γ". Improved cryogenic toughness has been oberved in several Fe-Ni alloys[3-5] heat treated in this way so as to retain some γ phase in bcc matrix. Therefore the effect of this treatment was investigated first in an Fe-12Mn-0.2Ti alloy.

As-quenched specimens were heated to various temperatures and held for 4 hours and then quenched. The amount of phases present in the cooled specimens was measured and plotted in Fig. 5 with corresponding Charpy impact energy at $-196^{\circ}C$. A significant variation of the amount of ε martensite and retained γ was observed in the specimens heat treated above $500^{\circ}C$. The maximum amount of ε martensite and retained γ was observed after $600^{\circ}C$ and 500 $550^{\circ}C$ treatment respectively. The maximum Charpy impact energy was obtained after $500^{\circ}C$ treatment although data scatter was rather significant. An evident correlation between the Charpy impact energy at $-196^{\circ}C$ and the amount of constitutent phases was observed in the specimens isothermally heat treated at $500^{\circ}C$. As shown in Fig. 6 the impact absorption energy increased with holding time at $500^{\circ}C$; so did the amount of retained γ in the specimen. On the other hand the increase of the vol. % of ε martensite was negligible

especially in the initial period, up to 4 hours.

Other mechanical properties were evaluated for the specimens reversion annealed for 8 hours at 500°C and the results are shown in Table III. A slight increase of yield strength over the as-quenched condition was observed. Rather substantial improvements of tensile ductility and fracture toughness (K_{IC}) were also observed. As shown in Fig. 7 the reversion annealed specimen showed improved ductile to brittle transition behavior in Charpy test. The fraction of intergranular fracture mode in a specimen broken at -196°C was approximately 50%.

The microstructures of a reversion annealed (500°C/8 hrs) 12Mn alloy are shown in Fig. 8(a) and (b). The optical micrograph, Fig. 8(a), is characterized by straightly aligned parallel interlath boundaries. The reverted γ phase was observed predominantly along these interlath boundaries as shown in the TEM micrograph, Fig. 8(b). It is noted that the interlath boundaries of the blocky martensites were often the location of ε martensite as shown in Fig. 3.

C. Fe-12Mn-0.2Ti. Effect of Cold Working on the Reversion Annealing Treatment.

A beneficial effect of combining cold working with the reversion annealing treatment was reported[12] in some Ni alloy steels and low Mn steels. The effect was expected to be greater in the 12Mn alloy steel because of the ε martensite intrusion. The cold working not only provides a strain energy for the higher decomposition rate of the metastable α martensite but also transforms the ε martensite to α martensite. It therefore removes the preferential nucleation sites for the reverted γ in the subsequent annealing.

The as-quenched blanks of 12Mn alloy were cold rolled 50% and reversion annealed at different temperature for 4 hours. The resultant phase distribution in the specimens and their Charpy impact energy at -196°C are shown in Fig. 9. Compared to the reversion annealing treatment alone (see Fig. 5) the combination of cold working and annealing resulted in greater amount

of retained γ and less amount of ε martensite. The correlationship between the amount of retained γ and the Charpy impact energy was excellent, showing the maximum values in the specimen annealed at 600°C.

Low temperature mechanical properties obtained for the specimens cold worked and annealed at 600°C for 4 hours are shown in Table III. An unusually high yield strength was obtained with a concomitant improvement of fracture toughness. In Charpy tests a sharp ductile-brittle transition was no longer observed as shown in Fig. 7. A fractograph of a specimen broken at -196°C, Fig. 10, did not show any trace of the brittle intergranular fracture. The microstructure of a cold worked and reversion annealed specimen, shown in Fig. 11, consisted of recrystallized α grains and uniformly distributed retained γ of slightly less than 0.5 μm.

D. Fe-12MN-0.2Ti. ε Martensite in the γ-Cycling Heat Treatment.

In a group of maraging steels it was observed[13-14] that a heat-cycling treatment between ambient temperature and above Afα resulted in an increase of fracture toughness. The improvement of the toughness was attributed to the accumulation of reverted γ which formed furing the slow heating across the two phase region. The accumulation of the reverted γ was also expected in the Fe-12Mn-0.2Ti alloy because of the broad two phase region. The application of above technique, however, resulted in some unusual effects in the 12Mn alloy.

The cycling treatment consisted of a repetition of a brief heating (5 min. at 680°C) and ice brine quencing cycle. As a result of this treatment a build-up of retained ε martensite rather than retained γ was observed as shown in Fig. 12. Saturation of the ε martensite occurred after three cycles. A small amount of retained γ was detectable within the first 5 cycles, but was absent after further cycling.

Mechanical properties were measured for the specimens γ-cycled five times and shown in Table III. A drastic reduction of the yield strength was observed

after the cycling treatment. On the other hand the ultimate tensile strength was slightly increased over as-quenched condition. A premature yielding phenomenon was observed in the engineering stress-strain curve. On the other hand, the γ-cycled specimens showed enhanced toughness in Charpy impact testing as shown in Fig. 7. The fracture surface of a Charpy specimen broken at -196°C, Fig. 13, showed a fibrous decohesion along prior γ grain boundaries rather than flat facets.

E. Fe-8Mn. Effect of Grain-Refining by γ, α + γ Cycling Heat Treatment.

Jin[6,15] developed a thermal cycling technique to reduce the grain size of an Fe-12Ni-0.25Ti alloy. The technique essentially utilizes the decomposition of the metastable α martensite in the two phase region and the homogenization/recrystallization reaction in γ region alternately. The effective reduction of grain size and the improvement of toughness by this technique has been also observed in other alloys.[16-17] However, a preliminary study to apply this technique to an Fe-12Mn-0.2Ti alloy was not successful. The reason appears to be the intrusion of the ε martensite, which will be discussed later. On the other hand the technique was found to be very effective in a 100% α martensitic Fe-8Mn alloy.

A schematic diagram of the heat treatment is shown in Fig. 14. An as-quenched specimen underwent a series of heat treatments consisting of 2 hours alternate holding in γ region and α + γ region of equilibrium phase diagram with intermittent quenching. The heat treating temperature in the γ region (750°C) was above Afα determined by dilatometry.

The reduction of grain size by the thermal cycling treatment is demonstrated in Fig. 15. Shown in Table III are the cryogenic tensile properties of the 8Mn alloy before and after the grain refinement. The 8Mn alloy had little ductility at -196°C in as-quenched condition. After the cycling heat treatment, however, the reduction in area was enhanced from 6% to 70% and

the total elongation was increased from 4% to 26%. The improved toughness was also evidenced in Charpy tests. As shown in Fig. 16 the transition temperature was suppressed from 30°C to -100°C.

The X-ray diffraction analysis showed that the 8Mn alloy grain-refined by the above method consisted of only bcc phase. In order to see the effect of retained γ in this structure an additional heat treatment (600°C/4h, denoted as 2B + Ret. γ in Fig. 14) was given to the heat cycled 8Mn alloy. Approximately 10 vol. % of retained γ and 9 vol. % of ε martensite was detected in the final specimen. This treatment resulted in an additional suppression of the transition temperature by 50°C. However this improvement of toughness was accompanied by a slight decrease in the yield strength as shown in Table III.

IV. DISCUSSION

A. Fe-12Mn-0.2Ti. Retained Phases.

The effect of equilibrium decomposition of α martensite within two phase (α + γ) region on resultant microstructure and mechanical properties has been extensively studied in Fe-Ni alloys.[3-5,18] Below Asα' the transformation is essentially diffusional process. The maximum rate of the γ reversion at given heat treating time and the retention of the reverted γ on subsequent cooling are determined by two factors; the slow kinetics of the transformation at low temperature and the low supersaturation of solute at high temperature. In the two phase decomposition the grain growth is inherently restricted by the impingement of the two crystallographically different phases.

A cold working process prior to the reversion annealing treatment significantly affects the amount of retained γ in final specimen. It not only provides strain energy to enhance the decomposition rate but also creates numerous defects for heterogeneous nucleation sites. Helped by the restricted grain growth this results in an extremely fine grain size. The reduction of grain size decreases Msα' of the reverted γ[19] thus increases the amount of retained γ in final structure.

The nature of the transformation in two phase region of equilibrium phase diagram of Fe-Mn system is similar to that of Fe-Ni alloys except for the intrusion of the ε martensite. Let us consider the case where the as-quenched structure is 100% α martensite. By the same reasoning in the Fe-Ni alloys one would expect the maximum content of retained γ in a sample heat treated at some intermediate temperature within the two phase range. In the Fe-Mn alloys an additional maximum must occur for ε martensite since the reverted γ may have a continuum of solute concentration with respect to heat treating temperature. The heat treating temperature for the maximum ε martensite is

higher than that for the maximum retained γ. If the as-quenched Fe-Mn alloy has already some ε martensite this would mostly affect the nucleation and growth pattern of reverted γ in subsequent two phase heat treatment because of a diffusionless transformation of $\varepsilon \rightarrow \gamma$ preceding the diffusional decomposition of $\alpha' \rightarrow \alpha + \gamma$.

As shown in Fig. 5 the maximum retention of the reverted γ and ε martensite in the reversion annealed Fe-12Mn-0.2Ti alloys occurs after 500~550°C and 600°C treatment respectively. The location of the ε martensite peak in Fig. 5 is in close agreement with Holden's[20] data which described a sharp maximum of ε content in Fe-15%Mn composition in binary alloys. According to an equilibrium phase diagram[21] the Mn concentration of the $\gamma/(\alpha + \gamma)$ boundary at 600°C is approximately 14%.

The initial presence of ε martensite in an as-quenched Fe-12Mn-0.2Ti alloy affects the resultant structure in a way to enhance the preferential growth of reverted γ. During heating the $\varepsilon \rightarrow \gamma$ diffusionless transformation occurs between 240°C and 350°C as shown in Fig. 1. The diffusional $\alpha' \rightarrow \alpha + \gamma$ transformation is active at least above 450°C. Consequently the growth of reverted γ in the latter reaction will occur most easily along the previously formed γ phase. This results in the unique lath-like microstructure shown in Fig. 8.

The cold working process added to the reversion annealing treatment changes the microstructure of Fe-12Mn-0.2Ti alloy in two ways: creating strain energy of the system and transforming ε martensite to α' martensite by a stress-assisted mechanism.[20,22-23] The effect of strain energy and defects is similar to that of Fe-Ni system. The $\varepsilon \rightarrow \alpha'$ transformation by cold working in Fe-Mn system is significant since it removes the origin of $\varepsilon \rightarrow \gamma$ reversion thus allows isotropic growth of new phases in $\alpha' \rightarrow \alpha + \gamma$ reaction. The increased amount of retained γ in contrast to the considerably reduced ε martensite

in Fig. 9 can be attributed to the grain size effect as in Fe-Ni system. Present data indicate that not only $M_{s\alpha'}$ but also $M_{s\varepsilon}$ temperature of reverted γ decreases with decreasing grain size.

The significance of the reversion annealing treatment from the mechanical property point of view is that it increases strength and toughness simultaneously. This is mainly due to the retained γ and the fine grain size. The impact toughness showed a particuarly good correlation with the amount of retained γ as shown in Fig. 6 and Fig. 9. From present data, however, it is difficult to isolate the contribution of the reduced grain size to the impact absorption energy from that of the retained γ phase. In Table III it is interesting to note that the yield strength of a reversion annealed specimen increased slightly from as-quenched state in spite of the presence of retained γ. This phenomenon may be attributed to the reduced grain size. Similar observations have been made in some other alloy steels[24-26] where a heat treatment causing a retention of reverted γ did not decrease the yield strength.

In contrast to the innocuous effect of the retained γ, the ε martensite seriously affects the yield strength of the 12Mn steel although it suppresses the ductile-brittle transition temperature. In a γ-cycled specimen almost 80 vol. % of ε martensite was detected while no significant change of the grain size or the amount of retained γ was observed. Therefore the decrease of yield strength in the γ-cycled specimen can be attributed to the ε martensite. The phenomenon is presumably due to the stress-assisted transformation of ε martensite to α' martensite, as was evidenced by a premature yielding in the tensile test. Therefore it may be concluded that the ε martensite is beneficial for the impact toughness of Fe-12Mn-0.2Ti alloy but with a sacrifice in yield strength.

B. Fe-8Mn. Grain Size Reduction by Thermal Cycling Technique.

The alternate heat cycling treatment between γ and $\alpha + \gamma$ region has been found effective in Fe-12Ni-0.25Ti,[6] Fe-8Ni-2Mn-0.25Ti[16] and 9Ni steel.[17] In present work the technique proved to be also effective in Fe-8Mn system. It is noted that the initial structure of these alloys is essentially 100% α' martensite with high dislocation density. The technique may not be so effective in an α' Mn steel alloy with an admixture of ε martensite as indicated by a preliminary study in an Fe-12Mn-0.2Ti alloy. The main reason appears to be the intrusion of $\varepsilon \rightleftarrows \gamma$ transformation into the $\alpha' \rightarrow \alpha + \gamma$ reaction as discussed before.

The extent of grain size reduction in the present work reasonably corresponds to the T_c suppression. When plotted according to Stroh's[27] relationship, T_c vs. ln (d), where T_c and d are the ductile to brittle transition temperature and the grain size respectively, a slope of $31^{\circ}C/\ln(\mu m)$ was obtained. This is in good agreement with Bolton's[8] and Roberts'[9] data in Fe-8Mn and Fe-9Mn respectively where the prior austentite grain size was controlled by different heat treating conditions in γ.

The T_c of the heat cycled specimen can be reduced further by additional heat treatement as shown in Fig. 16. However a slight degradation of yield strength is unavoidable in this case. This phenomenon may be attributed either to the retained γ or the ε martensite present in the final specimens. A conclusive evidence was not sought in this work. However, in view of the earlier observation on the role of the ε martensite in 12Mn alloy the cause would be more likely found in the premature yielding induced by the stress assisted $\varepsilon \rightarrow \alpha'$ transformation.

V. CONCLUSIONS

The following conclusions may be drawn from the present investigation.

(1) A reversion annealing heat treatment within the two-phase ($\alpha + \gamma$) region is beneficial for the low temperature mechanical properties of Fe-12Mn-0.2Ti steel. The improvement in properties is obtained mainly by retained austenite and grain size reduction.

(2) Cold-working enhances the improvement in the cryogenic mechanical properties produced by the reversion annealing treatment. This is achieved chiefly through an increase of the decomposition rate and the removal of preferential sites for the new phase. Combining the two processes results in a simultaneous improvement of toughness and yield strength in Fe-12Mn-0.2Ti steel.

(3) The presence of ϵ martensite suppresses the doctile-brittle transition temperature of Fe-12Mn-0.2Ti steel, but only at the expense of yield strength.

(4) An Fe-8Mn alloy can be toughened by a cycling heat treatment to reduce grain size. This technique is ineffective in an Fe-12Mn-0.2Ti alloy due to the presence of ϵ martensite in the initial structure.

ACKNOWLEDGMENT

The support of the National Aeronautics and Space Administration, Lewis Research Center under Contract No. NASA-NGR-05-003-562 and of the Materials and Molecular Research Division of the Department of Energy is gratefully acknowledged.

REFERENCES

1. W. Jolley: J. Iron Steel Inst., Feb., 1968, v. 206, p. 170.

2. W.C. Leslie, R.J. Sober, S.G. Babcock, and S.J. Green: Trans. ASM, 1969, v. 62, p. 690.

3. C.W. Marschall, R.F. Heheman, and A.R. Troiano: Trans. ASM, 1962, v. 55, p. 135.

4. S. Nagashima, T. Ooka, S. Sekino, H. Mimura, T. Fujishima, S. Yano, H. Sakurai: Trans. Iron Steel Inst. Japan, 1971, v. 11, p. 402.

5. S. Yano, H. Sakurai, H. Mimura, N. Wakita, T. Ozawa, and K. Aoki: Trans. Iron Steel Inst., Japan, 1973, v. 13, p. 133.

6. S. Jin, J.W. Morris, Jr., and V.F. Zackay: Met. Trans. A, 1975, v. 6A, p. 141.

7. S.K. Hwang, S. Jin, and J.W. Morris, Jr.: Met. Trans. A, 1975, v. 6, p. 2015.

8. J.D. Bolton, E.R. Petty, and G.B. Allen: Met. Trans., 1971, v. 2, p. 2915.

9. M.J. Roberts: Met. Trans. 1970, v. 2, p. 3287.

10. M.J. Schanfein, M.J. Yokota, V.F. Zackay, E.R. Parker, and J.W. Morris, Jr.: ASTM STP 579, 1975, p. 361.

11. B. Miramon: M.S. Thesis, UC Berkeley, Sept. 1967, UCRL-17849.

12. R.L. Miller: Met. Trans., 1972, v. 3, p. 905.

13. A.Goldberg: Trans. ASM, 1968, v. 61, p. 26.

14. S.D. Antolovich, A. Saxena, and G.R. Chanani: Met. Trans., 1974, v. 5, p. 623.

15. S. Jin, S.K. Hwang, and J.W. Morris, Jr.: Met. Trans. A, 1975, v. 6A, p. 1569.

16. S. Jin, S.K. Hwang, and J.W. Morris, Jr.: Met. Trans. A, 1975, v. 6A, p. 1721.

17. C.K. Syn, S. Jin, and J.W. Morris, Jr.: Met. Trans. A, 1976, v. 7A, p. 1827.

18. H. Haga: Trans. Iron Steel Inst. Japan, 1973, v. 13, p. 141.

19. W.C. Leslie, and R.L. Miller: Trans. ASM, 1964, v. 57, p. 972.

20. A. Holden, J.D. Bolton, and E.R. Petty: J. Iron Steel Inst., Sept., 1971, v. 209, p. 721.

21. M. Hansen: "Constitution of Binary Alloys" 2nd edition, McGraw-Hill, 1958, p. 664.

22. V.F. Zackay, E.R. Parker, D. Fahr, and R. Bush: Trans. ASM, 1967, v. 60, p. 252.

23. B. Cina: Acta Met., 1958, v. 6, p. 748.

24. D.T. Peters: Trans. ASM, 1968, v. 61, p. 63.

25. C.A. Pampillo, and H.W. Paxton: Met. Trans., 1972, v. 3, p. 2895.

26. D.T. Peters and C.R. Cupp: Trans. TMS-AIME, 1966, v. 236, p. 1420.

27. A.N. Stroh: Advan. Pys., 1957, v. 6, p. 418.

Table I. Chemical Composition of Alloys.

Alloy Designation	Composition (wt. pct)											
	Fe	Mn	Ti	C	O	S	P	Mo	Ni	Cr	V	Nb
Fe-8Mn	Bal.	7.8	0.04	0.002	0.050	0.006	0.007	-	-	-	-	-
Fe-12Mn-0.2Ti	Bal.	11.9	0.16	0.001	0.028	0.007	0.007	0.010	0.050	0.002	0.010	0.005

- : Not analyzed

Table II. Transformation Temperatures (^{o}C) of Alloys.

Alloy Designation	Asε	Afε	Asα'	Afα'	Msα'	Mfα'
Fe-8Mn	-	-	660	700	460	310
Fe-12Mn-0.2Ti	240	350	570	670	260	120

Asε, Afε: Start and finish temperature for $\varepsilon \rightarrow \gamma$ transformation on heating.

Asα', Afα': Start and finish temperature for $\alpha' \rightarrow \gamma$ transformation on heating.

Msα', Mfα': Start and finish temperature for $\gamma \rightarrow \alpha'$ transformation on cooling.

Table III. Mechanical Properties of Fe-Mn Alloys.

Composition	Treatment	Test Temp.(^{o}C)	σ_{y} (MNm^{-2})	σ_{uts} (MNm^{-2})	Uniform Elong.(%)	Total Elong.(%)	Red. in Area(%)	K_{IC} ($MNm^{-3/2}$)
Fe-12Mn-0.2Ti	As-Quenched	25	600	924	6	25	78	-
"	"	-196	889	1351	11	25	54	63
"	500^{o}C/8 hrs	-196	952	1358	18	33	62	70
"	50% reduction +600^{o}C/4 hrs	-196	1179	1503	26	38	66	100
"	680^{o}C/5min., 5 cycle	-196	593	1393	19	33	61	79*
Fe-8Mn	As-Quenched	-196	965	1041	4	4	6	-
"	750^{o}C/2hrs +650^{o}C/2hrs, 2 cycles	-196	965	1055	26	7	70	-
"	Above + 600^{o}C/4 hrs	-196	848	1083	32	18	64	-

- : not measured

* : K_{Q} value. ASTM thickness requirement for K_{IC} was not met.

σ_{y}: 0.2% offset engineering yield strength.

σ_{uts}: Ultimate tensile strength.

FIGURE CAPTIONS

Fig. 1. Fe-12Mn-0.2Ti. A dilation curve showing transformation temperatures during continuous heating and cooling.

Fig. 2. TEM (Transmission Electron Microscopy) micrographs of as-quenched structures.
(a) Fe-8Mn
(b) Fe-12Mn-0.2Ti

Fig. 3. TEM dark field image of ε martensite with diffraction pattern analysis. The image was obtained by $(10\bar{1}0)\varepsilon$ reflection.

Fig. 4. SEM (Scanning Electron Microscopy) micrographs of fracture surfaces of Charpy specimens broken at -196°C.
(a) Fe-8Mn
(b) Fe-12Mn-0.2Ti

Fig. 5. Fe-12Mn-0.2Ti. Structural constituents and Charpy impact energy (CVN) at -196°C of the specimens heat treated at temperatures for 4 hours.

Fig. 6. Fe-12Mn-0.2Ti. Structural constituents and Charpy impact energy (CVN) at -196°C of the specimens heat treated at 500°C for indicated period.

Fig. 7. Fe-12Mn-0.2Ti. Ductile to brittle transition curves after different treatments.
As-quenched; austenitizing (900°C/2hrs)
Reversion annealed; 500°C/8hrs
γ-cycled; 680°C/5min., 5 cycles
Cold work (50%) + Reversion annealing; 50% Reduction +600°C/4hrs

Fig. 8. Fe-12Mn-0.2Ti. Optical (a) and TEM (b) micrographs of a reversion annealed specimen (500°C/8hrs)

Fig. 9. Fe-12Mn-0.2Ti. Structural constituents and Charpy impact energy (CVN) at -196°C of the specimens cold worked 50% and annealed at temperature for 4 hours.

Fig. 10. Fe-12Mn-0.2Ti. SEM micrograph of fracture surface of a Charpy specimen broken at -196°C. Treatment; 50% cold reduction and annealed at 600°C for 4 hours.

Fig. 11. Fe-12Mn-0.2Ti. Optical (a) and TEM (b) micrographs of a specimen cold worked 50% and annealed at 500°C for 8 hours.

Fig. 12. Fe-12Mn-0.2Ti. Variation of structural constituents upon γ-cycling heat treatment (680°C/5min.)

Fig. 13. Fe-12Mn-0.2Ti. SEM micrograph of fracture surface of a Charpy specimen broken at -196°C. Treatment; γ-cycling heat treatment (680°C/5min., 5 cycles).

Fig. 14. Fe-8Mn. A schematic diagram of γ, α + γ cyclling heat treatment for grain refining.
Treatment; 750°C/2hrs (1A,2A) and 650°C/2hrs (1B,2B), 2 cycles.
Additional heat treatment (600°C/4hrs) was added for 2B + Ret.γ.

Fig. 15. Fe-8Mn. Optical micrographs of an as-quenched specimen (a) and a γ, α + γ cycling heat treated specimen (b). The structure of (b) was obtained after 2B treatment in Fig. 14.

Fig. 16. Fe-8Mn. Ductile to brittle transition curves after different heat treatments. See Fig. 14 for the heat treatments schematic.

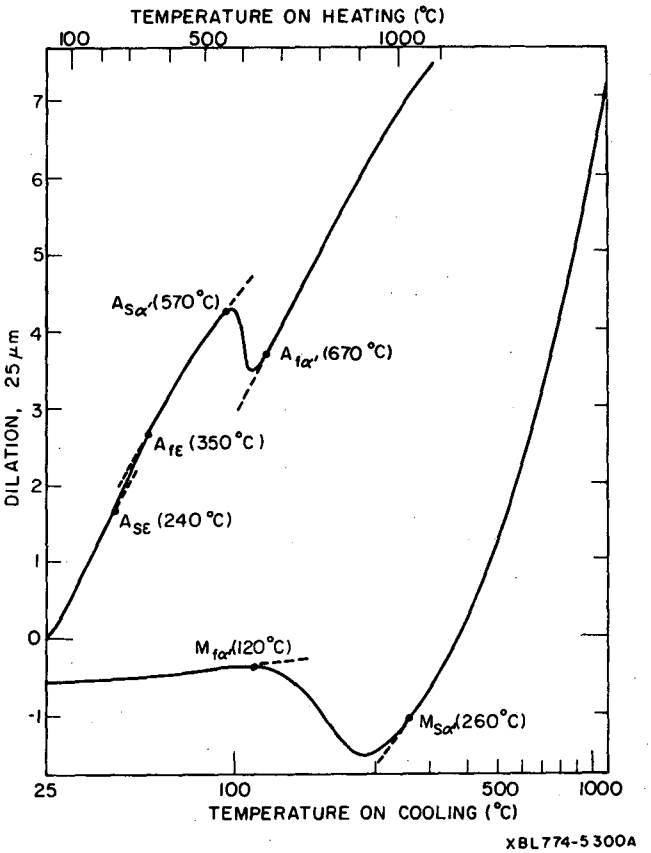
TEMPERATURE ON HEATING (°C)
100
500
1000
7
6
5
4
3
2
1
0
-1
DILATION, 25 μm
$A_{S\alpha'}$ (570°C)
$A_{f\alpha'}$ (670 °C)
$A_{f\varepsilon}$ (350 °C)
$A_{S\varepsilon}$ (240 °C)
$M_{f\alpha'}$ (120°C)
$M_{S\alpha'}$ (260°C)
25
100
500
1000
TEMPERATURE ON COOLING (°C)
XBL774-5300A

Fig. 1

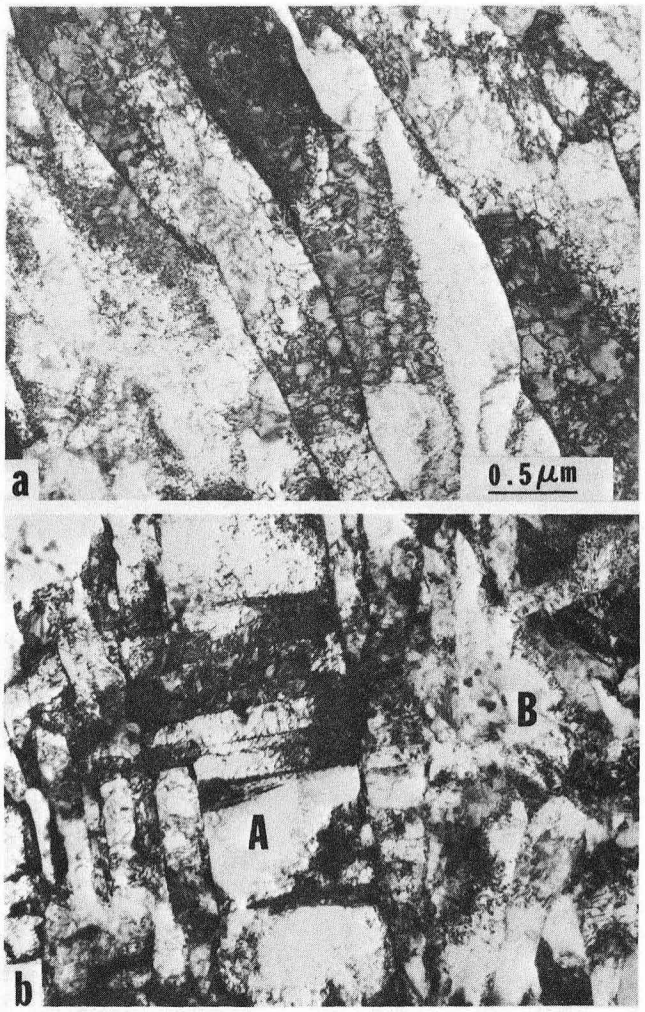

XBB 782-2101

Fig. 2

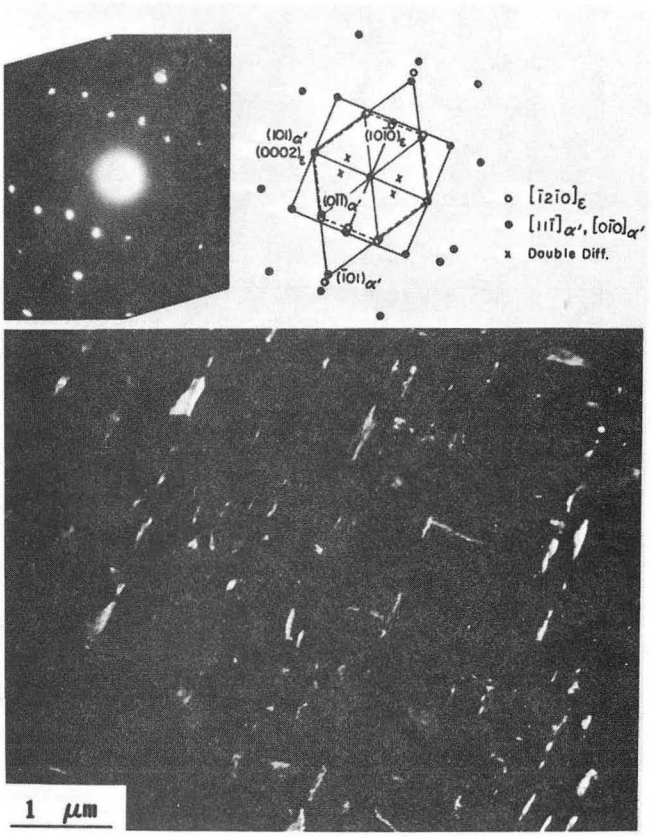

XBB 781-764

Fig. 3

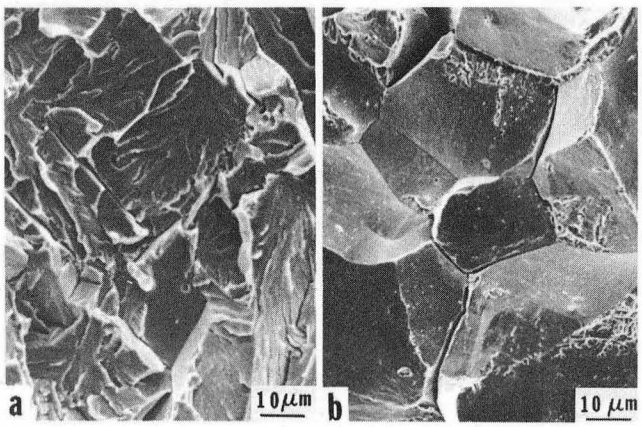

XBB 782-1661

Fig. 4

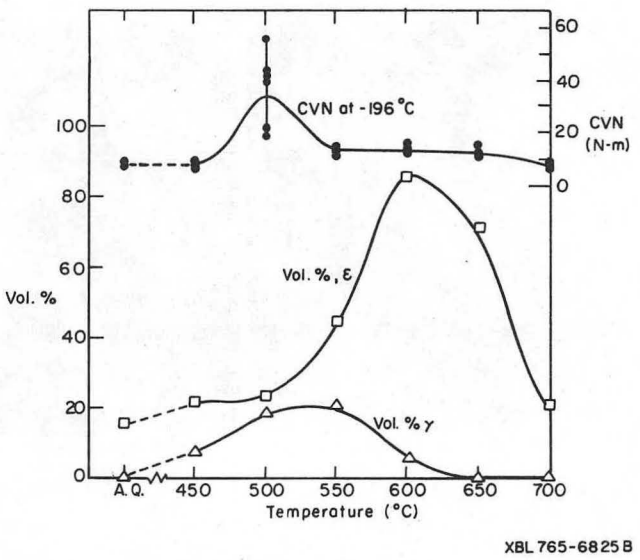
CVN at -196°C
Vol. %, ε
Vol. % γ
Vol. %
CVN (N-m)
Temperature (°C)
A.Q.
450
500
550
600
650
700
0
20
40
60
80
100
XBL 765-6825 B

Fig. 5

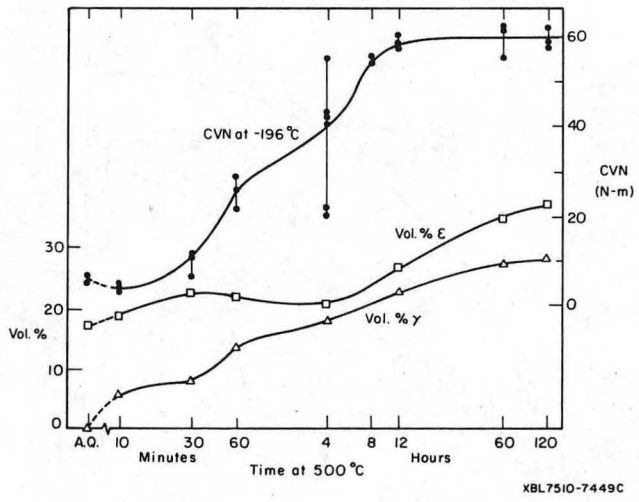

Fig. 6

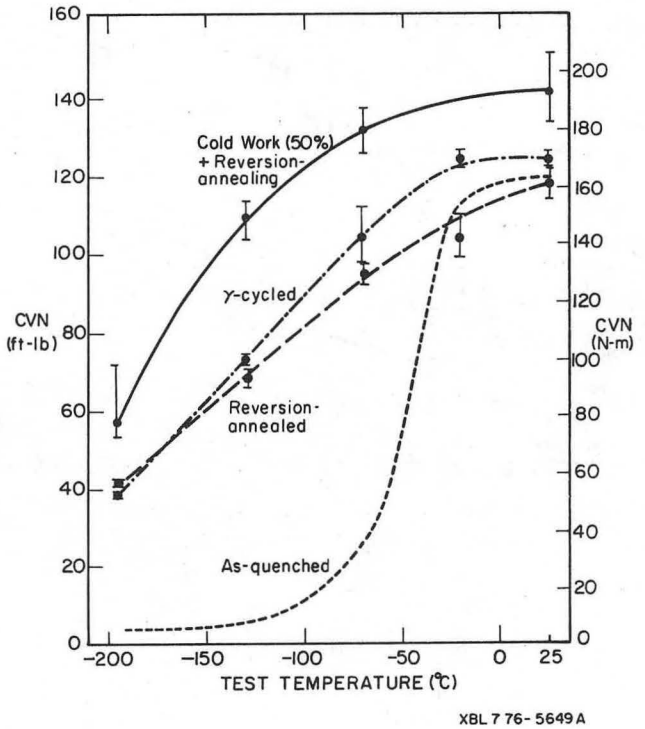
160
140
120
100
80
60
40
20
0
CVN
(ft-lb)
200
180
160
140
120
100
80
60
40
20
0
CVN
(N-m)
Cold Work (50%)
+ Reversion-
annealing
γ-cycled
Reversion-
annealed
As-quenched
-200
-150
-100
-50
0
25
TEST TEMPERATURE (°C)
XBL 776-5649A

Fig. 7

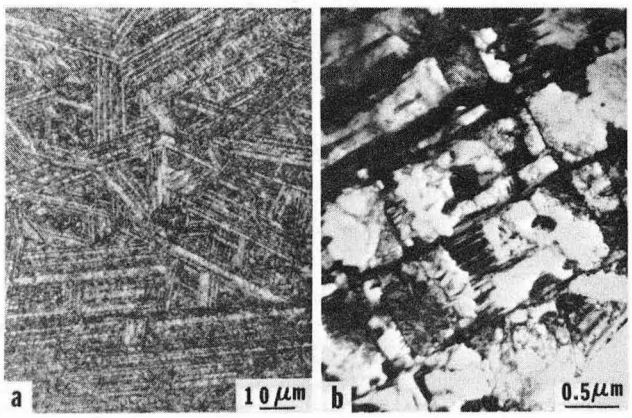

XBB 781-763

Fig. 8

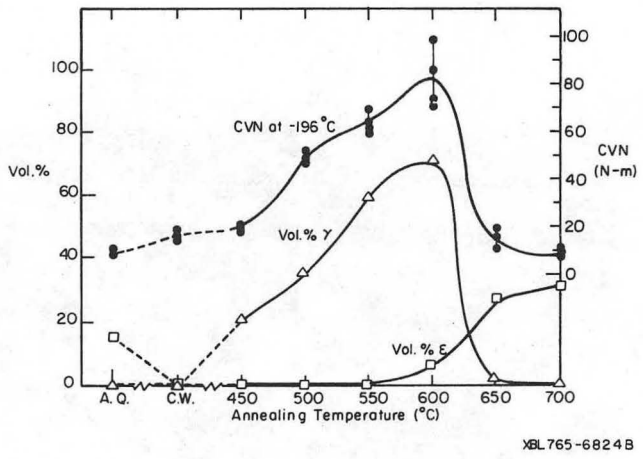
Vol.%
CVN (N-m)
CVN at -196°C
Vol.% γ
Vol.% ε
A.Q.
C.W.
450
500
550
600
650
700
Annealing Temperature (°C)
XBL765-6824B

Fig. 9

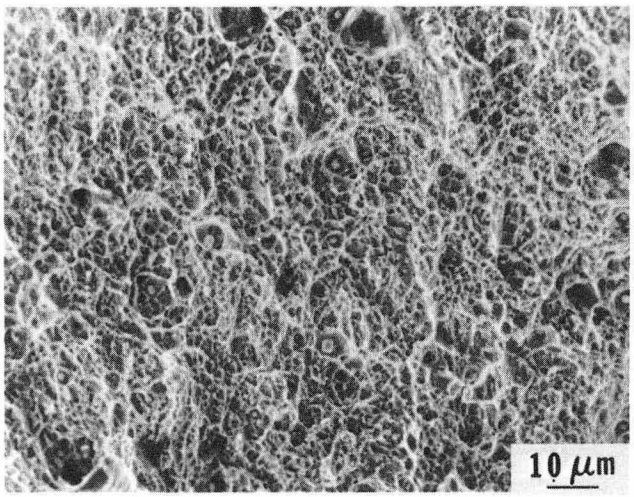

XBB 782-1658

Fig. 10

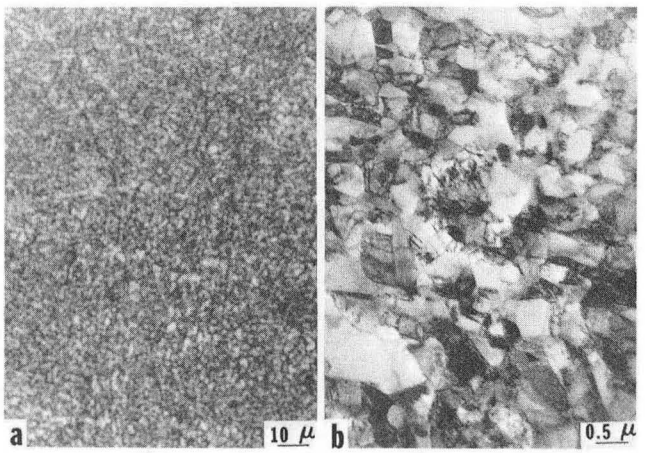

XBB 782-1659

Fig. 11

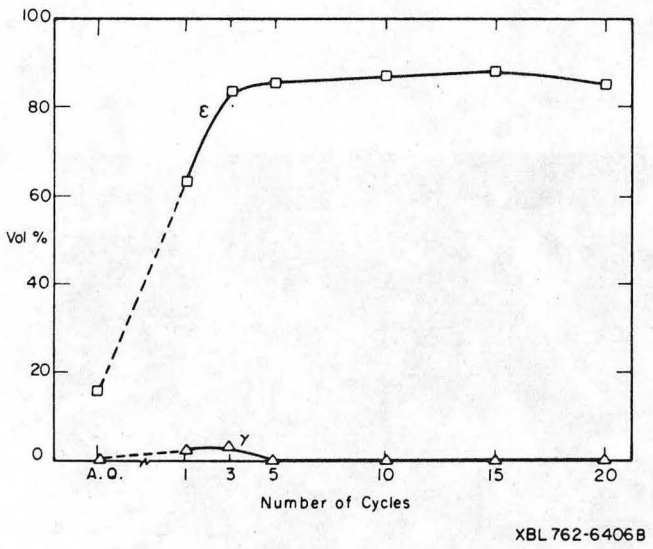

Fig. 12

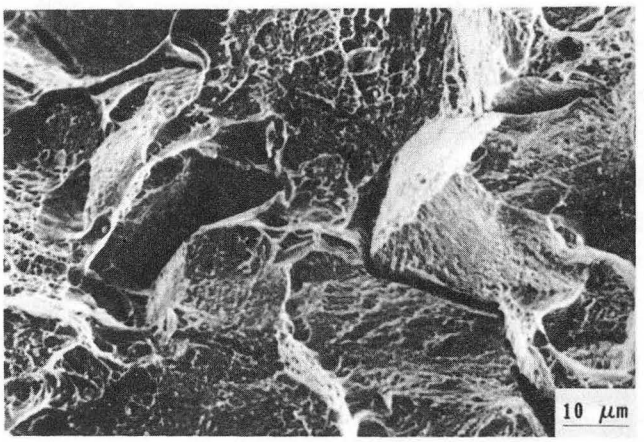

XBB 774-3177

Fig. 13

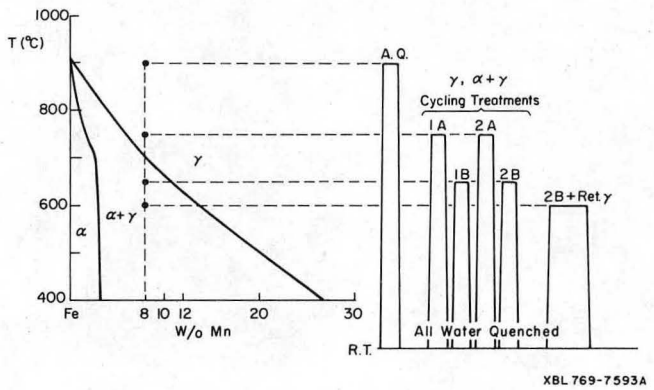

Fig. 14

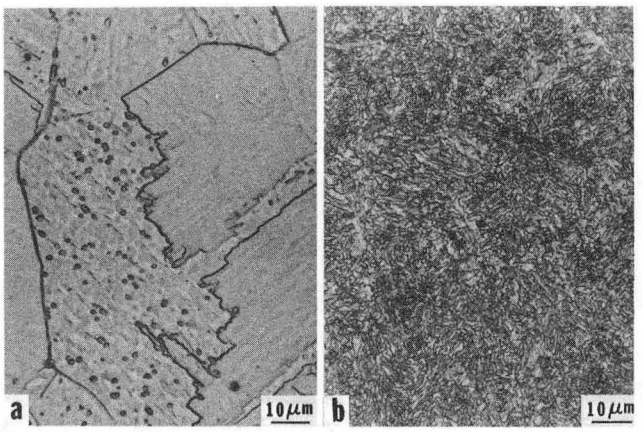

XBB 782-1660

Fig. 15

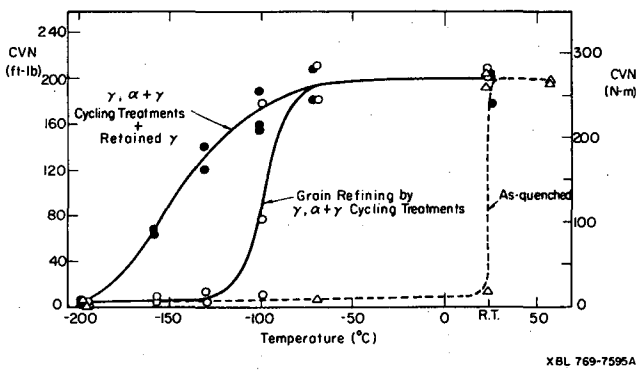
CVN
(ft-lb)
240
200
160
120
80
40
0
CVN
(N-m)
300
200
100
0
γ, α+γ
Cycling Treatments
+
Retained γ
Grain Refining by
γ, α+γ Cycling Treatments
As-quenched
-200
-150
-100
-50
0
R.T.
50
Temperature (°C)
XBL 769-7595A

Fig. 16

TECHNICAL INFORMATION DEPARTMENT
LAWRENCE BERKELEY LABORATORY
UNIVERSITY OF CALIFORNIA
BERKELEY, CALIFORNIA 94720